IEEE Access
Multidisciplinary ⋮ Rapid Review ⋮ Open Access Journal

Received 17 February 2023, accepted 15 March 2023, date of publication 20 March 2023, date of current version 23 March 2023.

Digital Object Identifier 10.1109/ACCESS.2023.3259100

RESEARCH ARTICLE

An Effective WBC Segmentation and Classification Using MobilenetV3–ShufflenetV2 Based Deep Learning Framework

BAIRABOINA SAI SAMBASIVA RAO AND BATTULA SRINIVASA RAO
School of Computer Science and Engineering, VIT-AP University, Amaravati, Andhra Pradesh 522237, India
Corresponding author: Battula Srinivasa Rao (srinivas.battula@vitap.ac.in)

ABSTRACT White Blood Cells are essential in keeping track of a person's health. However, the pathologist's experience will determine how the blood smear is evaluated. Furthermore, it is still challenging to classify WBCs accurately because they have various forms, sizes, and colors due to distinct cell subtypes and labeling methods. As a result, a powerful deep learning system for WBC categorization based on MobilenetV3-ShufflenetV2 is described in this research. Initially, the WBC images are segmented using an efficient Pyramid Scene Parsing Network (PSPNet). Following that, MobilenetV3 and an Artificial Gravitational Cuckoo Search (AGCS)-based technique are used to extract and select the global and local features from the segmented images. Finally, the WBC images are divided into five classes using a ShufflenetV2 model. The proposed approach is evaluated on blood cell count and detection (BCCD) and Raabin-Wbc datasets and achieves 99.19% and 99% accuracy, respectively. Moreover, the results are satisfactory when compared to existing algorithms.

INDEX TERMS White blood cells, deep learning, mobilenetV3, shufflenetV2.

I. INTRODUCTION

Infection illnesses continue to rank as one of the most complex problems in public health after decades of research and effort. As stated by the World Health Organization (WHO), viral infections are currently the deadliest communicable illness in the world and the fourth most significant reason for death in people [1], [2], [3]. They are some of the biggest global issues, affecting people, society, and the economy everywhere. To address this widespread, potentially fatal problem, it is crucial to build reliable techniques for early diagnosis and look into the pandemic's origin.

The peripheral blood smear is a typical laboratory test that gives much information about a patient's overall status to the doctor. It offers a statistical and qualitative evaluation of blood constituents, primary cells, and platelets. Human blood comprises three types of blood cells [4], [5], [6], [7]. They are leukocytes (WBC), erythrocytes (red blood cells), and thrombocytes (platelets). The Hosseinimost prevalent blood cells are erythrocytes, which contain the hemoglobin protein that gives the cell its red color. Leukocytes are agranular, colorless cells with a variable number of nuclei encircled by a small amount of cytoplasm. There are lots of leukocytes in the lymphatic system. They function as an essential component of the immune system in the blood, guarding the body against communicable diseases and outside invaders [8], [9], [10]. Thrombocytes, often known as platelets, are comparatively smaller than erythrocytes and lack a nucleus.

Lymphocytes, neutrophils, eosinophils, basophils, and monocytes are the five different types of nucleated cells that make up leukocytes [11], [13], [23]. Pathologists will be able to identify a variety of blood illnesses and diseases, such as anemia, leukemia, and malaria, with the correct and exact identification, counting, and categorization of WBC and the variation in percentage between the subtypes [14], [15], [16]. Better knowledge will aid in treatments, prevent harmful drug interactions, and monitor the patient's health.

The associate editor coordinating the review of this manuscript and approving it for publication was Wenming Cao.

Pathologists perform manual WBC identification, which is frequently prone to human error and yield unreliable results. Pathologists may do this procedure differently inside and across classes, which makes it tiresome and time-consuming [17], [18]. In the traditional WBCs identification system, the classification of WBC from other blood components is difficult due to their similar textures and uneven boundaries. Additionally, WBCs have a complex range of color, structure, form, and intensity [19], [20]. Different staining and lighting conditions also make it more challenging to identify WBC. Furthermore, the multi-class categorization adds to the complexity of the entire system and takes up a lot of processing time. For the reasons listed above, the standard technique fails to capture the accurate pathologist level of knowledge in the detection of WBCs, lacks robustness, and only performs well on small datasets under controlled circumstances.

Motivated by these observations, this paper presents an effective deep learning based framework for the recognition and categorization of WBCs. Specifically, Pyramid Scene Parsing Network (PSPNet) incorporates several pooling layers to maximize the global context and various layers links to have diverse segmentation layouts. Moreover, MobilenetV3 uses a partial residual design to boost the ability of features to reveal themselves, and its bottleneck architecture reduces the loss of low-dimensional characteristics. The ShuffleNetV2 based classifier reduces computing costs while retaining accuracy using channel shuffle and pointwise group convolution. Moreover, its efficient feature reuse mode is tremendously advantageous to the proposed framework. These advantages of both PSPNet, MobilenetV3, and ShuffleNetV2 make the proposed model more robust and classify the WBC more efficiently images into monocytes, basophils, eosinophils, neutrophils, and lymphocytes classes.

A. OUR CONTRIBUTIONS

1) The most effective segmentation and classification techniques are used to create the WBC classification model.
2) An effective mobilenetV3 network is implemented to extract global and local features from the image. From that, the optimal features are chosen using the Artificial Gravitational Cuckoo Search (AGCS) algorithm, which improves the classifier's performance.
3) Many experiments are run on the BCCD and Raabin-WBC datasets using various performance indicators to assess the proposed approach's performance.

The remaining proportion of the proposed article is organized as follows: Section II presents the background information and literature on the suggested model. Section III presents the suggested framework model, while Section IV presents the findings and discussions. The conclusion is shown in Section V.

II. LITERATURE REVIEW

It is quite tricky to identify WBC because of its diversity. Numerous researchers have looked into various methods in this area. The following discusses a few of them.

To categorize five different types of WBC using microscopic images, Manthouri et al. [21] developed a system for blood samples. To separate the nuclei from the input image, the Gram-Schmidt algorithm was employed in this system. The most predictable features were then extracted using Scale-Invariant Feature Transform based technique. A convolutional neural network (CNN) was implemented to learn contextual dependencies while maintaining spatial neighborhood dependencies. The authors employed the weighted two-phase test sample sparse representation technique for classification. WBC and LISC datasets were utilized to evaluate the efficiency of the suggested approach.

By combining many datasets from different sources, Cheuque et al. [22] presented a multilevel CNN framework to enhance the recognition and categorization of individual WBC. The Faster R-CNN network was used at the first level to distinguish between mononuclear and polymorphonuclear cells in identifying the region of interest for WBC. To categorize the subcategories in the second level, two parallel CNN models were implemented. The MobileNet architecture was the foundation for the implementation of the ML-CNN proposal. Additionally, the MobileNet utilized the depthwise separable convolution to fetch pertinent characteristics from every channel, making greater use of the data present in the images for leukocyte categorization. For performance assessment, LISC, KBC, WBC, CBC, and BCD datasets were used.

To automatically categorize WBC subclasses based on focalized attention mechanism, Wang et al. [23] introduced the Deep CNN with feature fusion techniques called WBC-AMNet. Gather-Excite (GE) and Squeeze-and-Excitation (SE) phases were combined in a focalized attention method to retrieve the fusion characteristics of the first and last convolutional layers of CNN to achieve more targeted attention. This study examines the effectiveness of classification performance using several metrics such as F1-score, precision, specificity, and accuracy on the WBC and BCCD datasets.

Alharbi et al. [24] suggested a technique that segments leukocytes from blood samples after extracting features from them using the ResNet and UNet networks. Using the semantic segmentation method, WBC segmentation was done for blood pictures using the MASK-RCNN network. Feature fusion, feature extraction, and Feature reconstruction were carried out in the U-net. However, due to the deep layer network's huge layers, gradient descent will occur when extracting features from the network. The authors applied the ResNet model to resolve these problems. The dice similarity coefficient (DSC), intersection-over-union (IoU), and the mean were utilized to evaluate the effectiveness of the approach.

Using the 4B-AdditionNet CNN architecture, Shahzad et al. [25] demonstrate how to classify WBC data. The input images were subjected to contrast-limited adaptive histogram equalization (CLAHE) during preprocessing. In addition to ResNet50 and EfficientNetB0 networks, a CNN was built and trained specifically for feature extraction. Ant colony optimization was utilized to choose the optimal characteristics. Then it was combined and sent to classifiers such as the quadratic discriminant analysis and support vector machine for categorization. For performance evaluation, the author used several evaluation criteria, including precision, F1 Score, sensitivity, and accuracy.

An approach based on deep learning was presented by Roy and Ameer [15] for segmenting leukocytes from microscopic blood images. The suggested model uses the DeepLabv3+ technique for segmentation and ResNet-50 for feature extraction. The following variables were chosen to evaluate the effectiveness of the suggested system: relative distance error, overall error rate, under-segmentation rate, over-segmentation rate, Dice similarity coefficient, mean IoU, mean accuracy, and mean BF score.

A system based on pretrained Alexnet and Googlenet architectures was presented by Cinar and Tuncer [26]. Preprocessing, filtering, feature extraction, and classification procedures were included in the suggested method. The Support Vector Machine classifies the feature vector that results from merging the feature vectors in the final pooling layers of both Alexnet and Googlenet techniques. This article handled two separate data sets from the LISC database and the Kaggle website to evaluate the proposed approach.

III. PROPOSED METHODOLOGY

This study intended to provide a new approach that is lighter, quicker, and more reliable than CNN-based techniques for categorizing white blood cells in peripheral smear pictures. Fig. 1 illustrates the proposed scheme's structure and stages. The first step is to obtain the appropriate test images from the database and finish the required data preprocessing. Following preprocessing, a PSPNet-based framework is used to segment the WBC nucleus from the image. Following that, using the MobilenetV3 and AGCS algorithms, the significant characteristics are retrieved, and more prominent features are chosen, respectively. The shufflenetV2 based network is implemented based on the final features chosen to classify the WBC into five classes: monocytes, basophils, eosinophils, neutrophils, and lymphocytes.

A. PREPROCESSING

During the preprocessing stage, the input images are resized into 256 × 256, and CLAHE is utilized on the images to increase contrast and highlight the cell bodies. An image augmentation technique was used on these blood cell images to reduce model overfitting, lessen data imbalance, increase validation accuracy, and improve discriminative performance. In particular, the picture dataset is improved by applying a color jitter modification (0.1) and flipping the image horizontally and vertically.

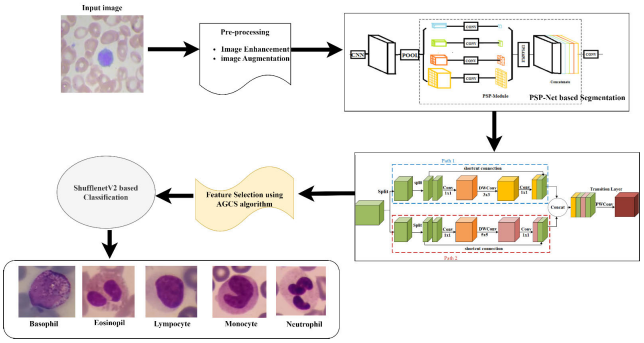

FIGURE 1. System architecture of the proposed approach.

B. PSPNet BASED SEGMENTATION

Following preprocessing, a PSP-net based network is used to separate the WBC nucleus from the picture. The PSPNet network structure is based on the residual network (ResNet) with some modifications. The suggested model has nine identity blocks, one max pooling layer, five convolution layers, three convolution blocks, three attention gates, and three pyramid pooling modules (PPMs). It is possible to incorporate the multiscale contexts by adding PPMs and merging multilayer characteristics by tightly integrating the PPMs in the decoder with the sub-sampling layers of the encoder. The performance of the suggested segmentation model is further enhanced by the application of an attention gate in the soft attention module.

To create feature maps FM with three distinct pyramid sizes, max pooling is first used, as shown in equation (1), where λ and DWS(.) are the inputs that represent the max pooling layer's strides and downsampling operations correspondingly. The sizes of the input and output feature maps, ip and op, are used in equation (2), which is used to calculate the max pooling layer's strides.

$$FM_k = DWS\left(FM, \lambda_k\right), \quad k = 1, 2, 3 \tag{1}$$

$$\frac{ip - \lambda_k}{\lambda_k} + 1 = op_k \Rightarrow \lambda_k = \frac{IS}{OS_k} \tag{2}$$

As illustrated in equation (3), bilinear interpolation is applied to scale the extracted features (OF) after the convolution operation on such multi-scale extracted features, where wt and bs are the weights and biases of the k^{th} 1×1 convolution layer, respectively, and $BI(.)$ is the bilinear interpolation operation.

$$OF_k = BI\left(wt_k \otimes FM_k + bs_k\right), \quad k = 1, 2, 3 \tag{3}$$

Furthermore, the original input and different pyramid scale's feature maps are concatenated. To decrease the channel number CH using equation (4), a 1×1 convolution operation is applied.

$$CH = wt_k\left(concat\left(FM, O_k\right)\right) + bs_k, \quad k = 1, 2, 3 \tag{4}$$

Here, bs_k and wt_k are bias and weights of the 1×1 convolution layer.

In max pooling, the original PPM generates the feature maps in four pyramid scales (1,2,3, and 6). In contrast to the original PPM, in our network, three pyramid scales feature maps (1,2, and 6) are produced by max pooling. For dimension reduction, a 1×1 convolution layer is also attached to the concatenation layer. Additionally, the fifth and third identity blocks and the first convolution layer's attention maps are generated using the first, second, and third attention gates correspondingly. Moreover, the outcomes of the attention gates and PPMs are tightly combined to integrate multilevel features. The final pixel-by-pixel prediction outcomes are obtained by feeding these integrated feature maps into a 1×1 convolution layer. In actual use, the PSPNet network has an auxiliary loss function to improve optimization outcomes.

C. MobilenetV3 BASED FEATURE EXTRACTION

This section presents detailed information about the implementation of MobileNetV3 used in our framework for WBC feature extraction. The method extracts the characteristics from a segmented image that is provided as input. Several bottleneck blocks make up the structure of MobileNetV3. The residual structure is one of the bottleneck blocks included in this network. There is just one path for feature extraction in the traditional bottleneck blocks which are replaced by the dual feature extraction paths in our approach called partial residual structure. This structure is used to lower the calculation cost of the residual framework.

A unique nonlinearity in MobileNetV3 is known as hard swish (hswish) which is a refined version of the sigmoid function. The h-swish nonlinearity is used to lessen the amount of training parameters and decrease the complexity of the model and size, which is expressed in Equation (5).

$$h - \text{swish}\,(x) = x.\sigma\,(x) \tag{5}$$

$$\sigma\,(x) = \frac{\text{ReLU6}\,(x+3)}{6} \tag{6}$$

Here, the piece-wise linear hard analog function is denoted as $\sigma\,(x)$.

Initially, the input image is given into the network's base layer that extracts initial features and forwards them into the bottleneck block. Then the input feature map is evenly split across two sections in the bottleneck block. One portion is utilized as the feature map input for path 1, and another is utilized as the feature map input for path 2. The input feature map is equally split into two portions in path 1. One portion is passed via a 1×1 convolution layer, 3×3 depthwise convolution layer, and 1×1 convolution layer. Through the shortcut connection, another path is straightly linked to the outcome of the residual learning section.

Similarly, in path 2, the input feature map is evenly split into two portions. In this 1×1 convolution layer, 5×5 depthwise convolution layer, and 1×1 convolution layer are all applied to one portion. One element of the output feature also uses the other directly. The output feature maps of two pathways are connected using the concatenation method. Finally, the transition layer is built to fuse the concatenated feature maps using a 1×1 pointwise convolutional kernel with batch normalization layer (BN) and ReLU or hswish activation functions.

D. FEATURE SELECTION USING AGCS ALGORITHM

The artificial gravitational cuckoo search (AGCS) algorithm is used in this work to choose features, which selects optimum features straightforwardly and easily. The newly developed cuckoo search algorithm operates in accordance with the required nest parasitism of cuckoo species. The cuckoo laid an egg in its nest; the strongest egg develops into the next generation. At least one egg is laid in the nest by the cuckoo during this phase to create the next generation. However, it can be challenging to select the best egg when the nest has multiple eggs. The best features must also be chosen from the collection of features. The characteristics are initially gathered in the feature space denoted by the expression $x = x_1, x_2, \ldots x_d$. Following the collection of all features, each feature is evaluated using the fitness function, which is carried out until the stop condition is reached (maximum number of features or max generation of cuckoo eggs). Before calculating the fitness function, the position of each feature in the feature space and its associated mass value, $ms(t)$, are established using the following equation.

$$ms_i\,(t) = \frac{fs(t) - wr(t)}{bs(t) - wr(t)} \tag{7}$$

Here, $fs(t)$ represents the fitness value, $wr(t)$ represents the worst features and $bs(t)$ represents the best features. The best and worst features are calculated using equations (8) and (9).

$$bs(t) = \min\left(fs_j(t)\right), j \in 1 \ldots .N \tag{8}$$

$$wr(t) = \max\left(fs_j(t)\right), j \in 1 \ldots .N \tag{9}$$

Then, the feature direction is calculated as well as the feature mass value as,

$$fd_j(t) = \frac{ms_i(t)}{\sum_{j=1}^{N} ms_i(t)} \tag{10}$$

The maximizing function is then used to define the fitness value of a feature. Once the effective features have been calculated based on the direction change and feature mass value, the features are selected to determine which features should be further optimized. The highly ranked characteristic that is selected as the best feature is used to process the classification of WBC. The improved classifier is then given the chosen features to carry out the recognition procedure.

E. SHUFFLENET V2 BASED CLASSIFICATION

ShuffleNet V2 is CNN based structure that is demonstrated to be quite effective in terms of computing. ResNet's residual architecture is optimized using channel shuffling and depthwise separable convolution, which not only increases the

model's operational efficiency but also ensures the network's accuracy. The input feature map is separated into X_1 and X_2 groups in the inverted residual module. In the X_2 path, the input passes through the depthwise separable convolution and two 1×1 convolution layers with the activation function and batch normalization. Afterward, the output of X1 and X2 feature maps are combined through the global pooling in the SE module.

There are two steps to it: the squeeze and excitation actions. Each channel's feature map is compressed by the Squeeze operation using global pooling, and each channel's weight can be obtained by the Excitation process. Afterward, the original feature map is multiplied by these weights in the Scale operation. To create two feature maps of mixed channel attention at various scales, the two-channel outcomes are multiplied by convolution 1 and convolution 2 in the channel dimension. The two feature maps are then added to create the output features.

A global pooled GP is used to flatten a feature map FE with a size of $x \times y$ and a total number of channels Cs into a feature vector of (1, 1, C) as shown below.

$$X_{cs} = GP(FE_{cs}) = \frac{1}{x \times y} \sum_{a=1}^{x} \sum_{b=1}^{y} FE_{cs}(a, b) \tag{11}$$

To increase the number of nonlinear circumstances and better account for the intricate channel correlation, the linear mapping and activation function is added to the feature vector. By dividing the estimated channel features by the original feature map, the channel attention result is then generated. The proposed framework's pseudocode and the proposed approach's step-by-step output are given in algorithm 1 and figure 2.

Algorithm 1

Input: BCCD and Raabin-WBC datasets
Initialize global and local/global variables and model parameters for training
    Train the network using the dataset
    PSPNet <——— Segment the WBC Nucleus.
    MobileNetV3 <——— Extract Global and local features.
    AGCS algorithm <——— Select Important features
    ShuffleNetV2 <——— Classify WBC subtypes
Return subtypes.

IV. RESULTS AND DISCUSSION

All of the outcomes from the suggested model are included in this section. On a desktop computer with an Intel Core (i7) 8700U processor running at 3.20 GHz, NVIDIA GeForce-GTX 1050 Ti graphics totaling 4 GB, and 16 GB of main memory, the experimental research for this paper was carried out. TensorFlow was used as the backend, and Python 3.7 was used to develop the software. In the experimental investigation, training data accounted for 70% of the data, while testing data made up 30%. All experiments use a batch size of 8,

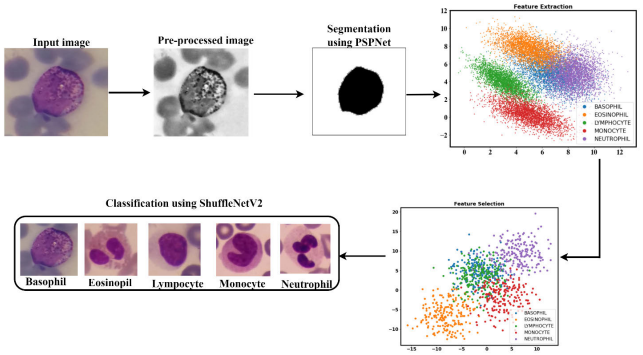

FIGURE 2. Step-by-step output of the proposed approach.

a learning rate of 0.001, a drop rate of 0.01, 100 epochs, an Adam optimizer, and an auxiliary loss function. The accuracy and error loss percentages show significant improvement from the beginning of the training and testing process until the end. The proposed approach's training and testing accuracies are 83.37% and 85.86%, respectively. Additionally, the suggested network's training and testing losses are 0.004 and 0.007. This training and testing study shows how well the proposed method could segment the input and learn features based on the available dataset to categorize the WBC.

A. DATASET DESCRIPTION

In our experiments, two different datasets are used for performance evaluation, including Raabin-WBC and BCCD.

1) BCCD DATASET

The BCCD dataset is publicly available. In this, 12,453 JPEG photos are available for leukocytes, and cell type labels are included in a CSV file. This dataset contains four cell types - neutrophil, monocyte, lymphocyte, and eosinophil - there are 3123, 3107, 3103, and 3120 augmented photos, as opposed to 207, 21, 33, and 88 original images. Since basophils typically comprise less than 1% of total leukocytes, they are not included in the dataset.

2) Raabin-WBC DATASET

The Raabin-WBC dataset is vast, and two hematologists have labeled every single row of data in it. It has 14514 WBC images with resolutions of 575×575, including 3461 lymphocytes, 8891 neutrophils, 795 monocytes, 301 basophils, and 1066 eosinophils. There are three sets in this dataset: Train, Test-A, and Test-B. Because the Test-B set has not yet been named, we did not utilize it. Cropped versions of the five abovementioned general categories of WBCs are included in the Train and Test-A sets.

B. SEGMENTATION RESULTS

1) PERFORMANCE METRICS FOR SEGMENTATION

The precision, sensitivity, and dice similarity coefficient (DSC) are measures used to assess the efficacy of the suggested nucleus segmentation algorithm. The following

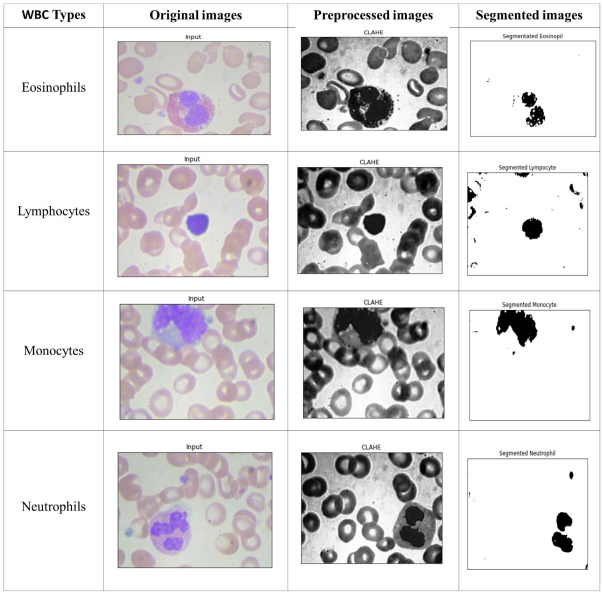

FIGURE 3. Segmented images of the BCCD dataset.

TABLE 1. Segmentation results of WBC classes in the BCCD dataset.

WBC cell type	DSC	Precision	Sensitivity
Neutrophils	98.83	99.89	99.92
Eosinophils	99.41	99.82	99.93
Monocytes	98.89	99.93	99.95
Lymphocytes	98.76	99.77	99.9

equations offer these metrics, which are generated using the segmentation's false negative (FsP), true negative (TrN), false positive (FsP), and true positive (TrP) values.

$$DSC = \frac{2 \times TrP}{2 \times TrP + FsP + FsN} \tag{12}$$

$$SEN = \frac{TrP}{TrP + FsN} \tag{13}$$

$$PPV = \frac{TrP}{TrP + FsP} \tag{14}$$

We employ both visual and numerical measurements to assess our suggested strategy. The results of segmenting the BCCD dataset are shown in Figure 3. The first column lists the input photographs, the second the outcomes of the preprocessing, and the third the segmented images.

The backdrop and the RBCs around the WBCs are erased from the image by the proposed approach, which performs exceptionally well in the majority of situations. Even when the form borders are unequal, our segmentation accurately isolates the nucleus regions. The four WBC subtypes were successfully segmented and recognized using the suggested approach; it was demonstrated (see Figure 3). Certain cells tightly spaced or situated at the margins could also be detected with reasonable accuracy.

Table 1 shows the derived DSC, Precision, and Sensitivity scores for each class in the BCCD dataset. The suggested

TABLE 2. Segmentation results of WBC classes in the Raabin-WBC dataset.

WBC cell type	DSC	Precision	Sensitivity
Neutrophils	98.78	99.85	99.89
Eosinophils	99.38	99.74	99.90
Monocytes	98.86	99.89	99.92
Lymphocytes	98.73	99.76	99.88
Basophils	98.71	99.73	99.83

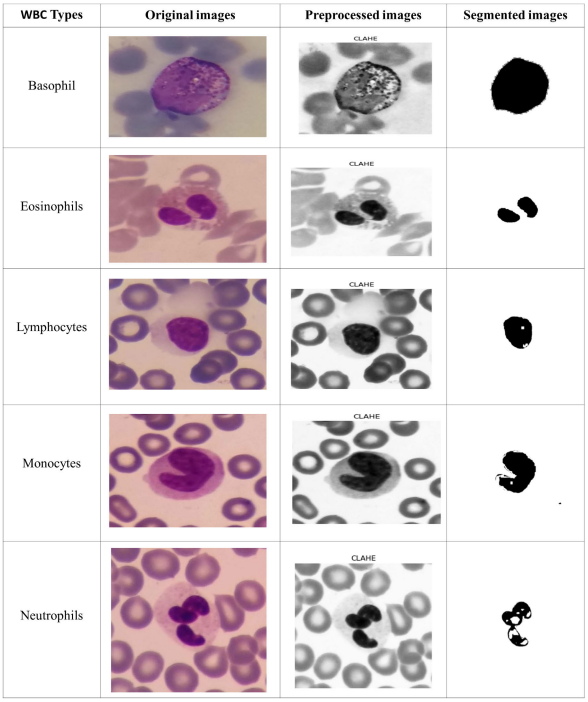

FIGURE 4. Segmented images of the Raabin-WBC dataset.

segmentation approach has minimal standard deviation for both DSC and accuracy, indicating that the approach consistently performs very well for different cells in the sample.

Figure 4 shows that the suggested method produces superior segmentation performance on the Rabbin-WBC dataset. The decision boundaries are pushed farther by using the auxiliary loss function to keep the optimization from stopping at a particular margin. This improves segmentation outcomes and enables the network to maintain strong generalization ability. Table 2 provides the quantitative outcomes of the suggested segmentation approach on the Raabin-WBC dataset.

The segmentation result of the suggested approach on the Eosinophils class is more significant than all other classes, with 99.38% DSC, 99.74% accuracy, and 99.9% sensitivity, as seen in Table 2. However, Monocytes achieve greater values than other groups in precision and sensitivity (99.89% precision and 99.92% sensitivity). The Basophils class scored slightly worse than the other classes in each of the five classes. It achieves a DSC of 98.71%, an accuracy of 99.73%, and a sensitivity of 99.83%.

TABLE 3. Classification results of four classes on the BCCD dataset.

WBC subtypes	DSC	Precision	Sensitivity	Specificity	F1-score
Monocytes	98.82	98.86	98.73	98.80	98.82
Eosinophils	98.69	98.75	98.65	98.69	98.70
Neutrophils	99.48	99.56	99.41	99.49	99.52
Lymphocytes	99.78	99.74	99.62	99.70	99.71

C. CLASSIFICATION RESULTS

1) PERFORMANCE METRICS FOR CLASSIFICATION

An essential step in creating a reliable classifier is assessing the effectiveness of a classification system. The most widely used evaluation metrics, including $F1$ Score, specificity, sensitivity, precision, and accuracy, are used in this work. Below is a list of the mathematical equations used in these techniques.

$$\text{Accuracy} = \frac{TrP + TrN}{TrP + TrN + FsP + FsN} \tag{15}$$

$$\text{Precision} = \frac{TrP}{TrP + FsP} \tag{16}$$

$$\text{Sensitivity} = \frac{TrP}{TrP + FsN} \tag{17}$$

$$\text{Specificity} = \frac{TrN}{TrN + FsP} \tag{18}$$

$$F1 - \text{Score} = \frac{2 \times \text{Precision} \times \text{recall}}{\text{Precision} \times \text{recall}} \tag{19}$$

Here, False Negative (FsN) indicates the number of blood cell types that were improperly identified, while True Positive (TrP) indicates the number of blood cell types that were correctly separated. The number of cells correctly detected as not being the target blood cell types is known as True Negative (TrN); False Positive (FsP) counts the number of cells mistakenly classified as the wrong type of blood cell.

2) CLASSIFICATION RESULTS ON THE BCCD DATASET

The categorization outcomes of the suggested approach utilizing the BCCD Dataset are reported in this section. It is clear from a careful examination of the F1-score criterion, which considers both precision and sensitivity, that our suggested approach has delivered the best results in most classes, as shown in Table 3. Overall, lymphocytes and neutrophils had the best classification impacts, while eosinophils displayed the worst ones. Since granulocytes such as neutrophils and eosinophils share a similar nucleus structure with other WBC categories, this difference was not statistically significant. Figure 5 shows a visual depiction of table 3 in a format. Based on every performance indicator, it can be seen from the figure that monocytes outperform eosinophils. In general, the suggested method minimizes the overall false- and leak-detection percentages, and the tracked bounds of the suggested method are highly accurate.

The proposed approach achieves 99.19% accuracy, 99.22% precision, 99.10% sensitivity, 99.17% specificity, and 99.18% f1-score, according to table 4. The findings of this

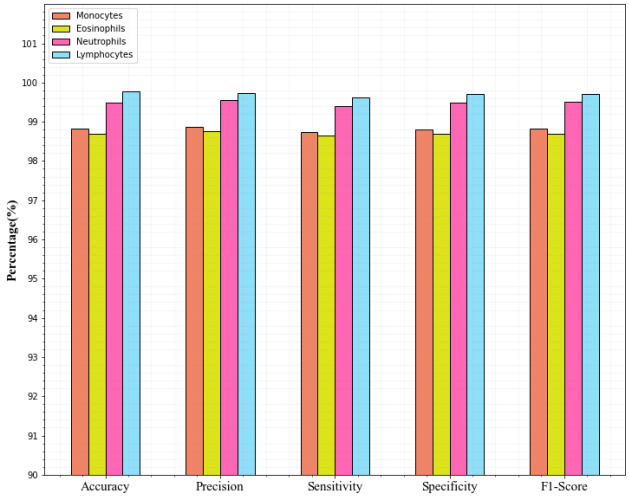

FIGURE 5. Graphical representation of four class classifications on the BCCD dataset.

TABLE 4. Comparison of the proposed approach on the BCCD dataset.

Techniques	DSC	Precision	Sensitivity	Specificity	F1-score
CSVM [25]	97.58	94.85	96.56	98.24	95.69
WBC-AMNet [23]	89.22	90.72	-	89.22	89.47
DenseNet121 [27]	94	94.22	93.74	-	93.81
CNN [19]	97	95	94	-	95
FIAL [2]	93.22	93	93	98	93.5
Proposed	99.19	99.22	99.10	99.17	99.18

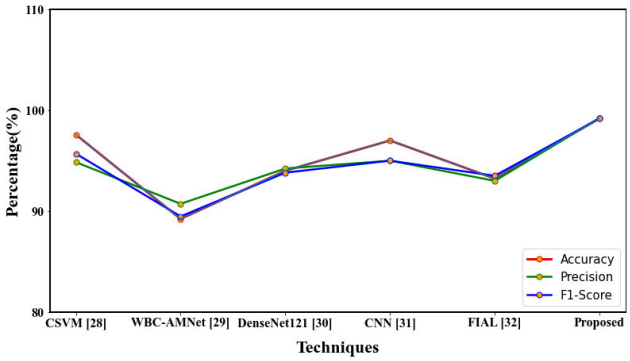

FIGURE 6. Comparison of classification results on the BCCD dataset.

study demonstrate that, in comparison to previous deeper networks, the suggested technique can be both sufficient and more successful in the WBC classification problem. Densenet-121's extensive connections increase the risk of overfitting by making networks more susceptible to computation and parameter inefficiency. When compared to the proposed method, Densenet-121 only achieves 94% accuracy. The performance of WBC-AMNet is relatively poor in comparison to all other networks. Only 89.22% accuracy and 90.72% precision are achieved. In contrast, Densenet-121 performs slightly better and achieves outcomes comparable to Fine-grained Interactive Attention Learning (FIAL). The graphical representation of this table is shown in figure 6.

TABLE 5. Classification results of five classes on the Raabin-WBC dataset.

WBC subtypes	DSC	Precision	Sensitivity	Specificity	F1-score
Monocytes	98.75	98.93	98.67	98.72	98.73
Eosinophils	98.61	98.72	98.59	98.61	98.68
Neutrophils	99.43	99.52	99.35	99.43	99.45
Lymphocytes	99.69	99.71	99.55	99.65	99.63
Basophils	98.54	98.69	98.47	98.56	98.62

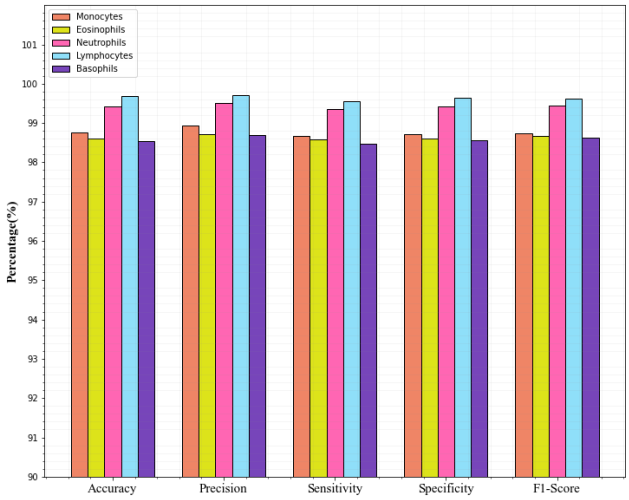

FIGURE 7. Graphical representation of five class classifications on the Raabin-WBC dataset.

3) CLASSIFICATION RESULTS ON THE RABBIN-WBC DATASET

The categorization outcomes of the suggested approach utilizing the Rabbin-WBC Dataset are reported in this section. The results of WBC's five class classifications are shown in table 5. The suggested method successfully recognized each class and produced improved results across the board. Our suggested method explicitly has a high f1-score (99.63%), sensitivity (99.55%), specificity (99.65%), and accuracy (99.69%) when classifying lymphocytes. The developed model more precisely extracts the characteristics of lymphocytes as contrasted to other categories. Eosinophils and Basophils have slightly lower accuracy than other classes due to a small percentage of them being incorrectly classified.

A summary of the outcomes for the various models-namely, Discriminative region detection assisted feature aggregation (DRFA-Net), Resnet-Densenet-SCAM, support vector machine (SVM), MID-YOLO, and our suggested method using Raabin-WBC dataset-is presented in Table 6. The findings are the sum of various measures, including F1-score, sensitivity, sensitivity, accuracy, and precision. In this dataset, our suggested method achieves 99% accuracy, 99.11% precision, 98.92% sensitivity, and 98.99% specificity. Figure 7 displays this table's graphical depiction.

Figure 8 shows that standard MID-YOLO and SVM perform quite poorly compared to alternative methods. Extensive WBC data make SVM unsuitable for handling them. When identifying eosinophils and monocytes, Yolo has significant misclassification issues, which leads to lower accuracy than other networks. The conclusion drawn from the preceding discussion is that the proposed technique can reliably and accurately carry out the process of WBC categorization.

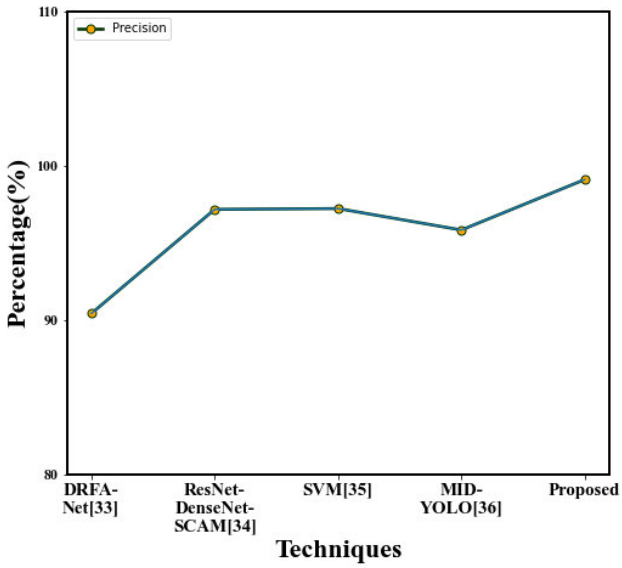

FIGURE 8. Accuracy comparison of the proposed approach on the Raabin-WBC dataset.

TABLE 6. Comparison of the proposed approach on the Raabin-WBC dataset.

Techniques	DSC	Precision	Sensitivity	Specificity	F1-score
DRFA-Net [28]	95.17	90.43	93.40	-	91.89
ResNet-DenseNet-SCAM [29]	98.71	97.18	98.42	-	97.78
SVM [30]	94.65	97.23	95.07	-	96.14
CNN [31]	93.97	-	-	-	-
Proposed	99	99.11	98.92	98.99	99

TABLE 7. Comparison of with and without feature selection technique.

With Feature selection					
Dataset	Accuracy	Precision	Sensitivity	Specificity	F1-score
BCCD	99.19	99.22	99.10	99.17	99.18
Raabin-wbc	99	99.11	98.92	98.99	99
Without Feature selection					
Dataset	Accuracy	Precision	Sensitivity	Specificity	F1-score
BCCD	99.03	99.13	98.98	99	99
Raabin-wbc	98.91	98.99	98.81	98.87	98.89

4) IMPACT OF FEATURE SELECTION

As was already noted, choosing the most robust features and training the learning algorithm with them can considerably minimize the size of the training, which significantly decreases the time and space complexity of the system. Because the feature selection approach enhances the classifier's performance, we examine its effectiveness in this section. Table 7 shows how feature selection has an impact.

This approach's performance has been significantly improved by the feature selection method based on the AGCS algorithm. It only achieves 99.03% accuracy for the BCCD dataset without feature selection and 98.91% accuracy for the raabin-WBC dataset. For complex classification tasks,

TABLE 8. Result of ANOVA test.

		df	Sum square	Mean square	f-value	p-value
Accuracy	Between groups	1	0.07896	0.07896	0.29	0.6069
	Within groups	7	1.9062	0.2723		
	Total	8	1.9852	0.2481		
Precision	Between groups	1	0.02863	0.02863	0.1233	0.7358
	Within groups	7	1.6252	0.2322		
	Total	8	1.6538	0.2067		
Sensitivity	Between groups	1	0.06923	0.06923	0.2917	0.6059
	Within groups	7	1.6614	0.2373		
	Total	8	1.7306	0.2163		

using optimization techniques for feature selection shows significant promise. In addition to improving performance, this strategy can reduce power and resource usage.

5) STATISTICAL ANALYSIS

The primary objective of this statistical analysis is to establish a specific degree of confidence in the suggested method. To verify whether the outcomes are statistically significant, we compare the means of a number of distributions using the analysis of variance (ANOVA) method.

Table 8 displays the statistical findings from the ANOVA test, including the degree of freedom (df), F-statistics, mean squared error (MSE), and p-value. It was considered to be significant when the probability value fell below 0.05. From the table, it is observed that p-value $> \alpha$. Therefore, all group averages are taken to be equal. In other words, there is not a substantial enough statistical difference between the averages of all groups.

6) LIMITATIONS OF THE PROPOSED FRAMEWORK

One of the shortcomings of the proposed structure is that we missed suppressing image noise. However, it did not significantly affect the performance of our proposed method. It is possible to remove image noise using techniques such as conservative smoothing, gaussian smoothing, unsharp filters, mean, a median, frequency filter, and others, which could improve the algorithm's performance. Moreover, to improve the classifier's performance, various optimization techniques like heuristics, metaheuristics, and Bayesian optimization may fine-tune the suggested technique's hyperparameters.

V. CONCLUSION

To help medical practitioners classify WBCs, this study aimed to employ a deep learning technique based on MobileNetV3-ShufflenetV2. Our framework is greatly improved by the partial residual structure of mobilenetV3, feature selection using the AGCS method, channel shuffle, and pointwise group convolution of shufflenetV3 networks and reach 99.19% and 99% accuracy for the BCCD and Raabin-wbc datasets, respectively. The suggested technique also has equally good segmentation ability and yields the best results. Moreover, the proposed approach outperforms the existing approaches in terms of performance on both datasets.

In future research, our suggested framework will also be tested in other areas, such as blood group identification, malaria parasite detection, anemia detection, leukemia detection, and RBC count with microscopic images. We can also concentrate on boosting the system's stability, reducing noise, and overall performance with effective preprocessing and post-processing phases.

REFERENCES

[1] A. Girdhar, H. Kapur, and V. Kumar, "Classification of white blood cell using convolution neural network," *Biomed. Signal Process. Control*, vol. 71, Jan. 2022, Art. no. 103156.

[2] Y. Ha, Z. Du, and J. Tian, "Fine-grained interactive attention learning for semi-supervised white blood cell classification," *Biomed. Signal Process. Control*, vol. 75, May 2022, Art. no. 103611.

[3] N. Dong et al., "A novel feature fusion based deep learning framework for white blood cell classification," *J. Ambient Intell. Hum. Comput.*, pp. 1–13, 2022, doi: 10.1007/s12652-021-03642-7.

[4] Q. Zhai, B. Fan, B. Zhang, J.-H. Li, and J.-Z. Liu, "Automatic white blood cell classification based on whole-slide images with a deeply aggregated neural network," *J. Med. Biol. Eng.*, vol. 42, no. 1, pp. 126–137, Feb. 2022.

[5] A. Meenakshi, J. A. Ruth, V. R. Kanagavalli, and R. Uma, "Automatic classification of white blood cells using deep features based convolutional neural network," *Multimedia Tools Appl.*, vol. 81, no. 21, pp. 30121–30142, 2022.

[6] R. Al-Qudah and C. Y. Suen, "Improving blood cells classification in peripheral blood smears using enhanced incremental training," *Comput. Biol. Med.*, vol. 131, Apr. 2021, Art. no. 104265.

[7] D. Ryu, J. Kim, D. Lim, H.-S. Min, I. Y. Yoo, D. Cho, and Y. Park, "Label-free white blood cell classification using refractive index tomography and deep learning," *BME Frontiers*, vol. 2021, Jan. 2021.

[8] J. Wu, X. Zheng, D. Liu, L. Ai, P. Tang, B. Wang, and Y. Wang, "WBC image segmentation based on residual networks and attentional mechanisms," *Comput. Intell. Neurosci.*, vol. 2022, pp. 1–13, Aug. 2022.

[9] M. Zhao, H. Yang, F. Shi, X. Zhang, Y. Zhang, X. Sun, and H. Wang, "MSS-WISN: Multiscale multistaining WBCs instance segmentation network," *IEEE Access*, vol. 10, pp. 65598–65610, 2022.

[10] E. Cengil, A. Çinar, and M. Yildirim, "A hybrid approach for efficient multi-classification of white blood cells based on transfer learning techniques and traditional machine learning methods," *Concurrency Comput., Pract. Exper.*, vol. 34, no. 6, p. e6756, Mar. 2022.

[11] A. Khan, A. Eker, A. Chefranov, and H. Demirel, "White blood cell type identification using multi-layer convolutional features with an extreme-learning machine," *Biomed. Signal Process. Control*, vol. 69, Aug. 2021, Art. no. 102932.

[12] Q. Wang, J. Wang, M. Zhou, Q. Li, Y. Wen, and J. Chu, "A 3D attention networks for classification of white blood cells from microscopy hyperspectral images," *Opt. Laser Technol.*, vol. 139, Jul. 2021, Art. no. 106931.

[13] M. Makem, A. Tiedeu, G. Kom, and Y. P. K. Nkandeu, "A robust algorithm for white blood cell nuclei segmentation," *Multimedia Tools Appl.*, vol. 81, no. 13, pp. 17849–17874, May 2022.

[14] A. Haider, M. Arsalan, Y. W. Lee, and K. R. Park, "Deep features aggregation-based joint segmentation of cytoplasm and nuclei in white blood cells," *IEEE J. Biomed. Health Informat.*, vol. 26, no. 8, pp. 3685–3696, Aug. 2022.

[15] R. M. Roy and P. M. Ameer, "Segmentation of leukocyte by semantic segmentation model: A deep learning approach," *Biomed. Signal Process. Control*, vol. 65, Mar. 2021, Art. no. 102385.

[16] D. Baby, S. J. Devaraj, and J. Hemanth, "Leukocyte classification based on feature selection using extra trees classifier: A transfer learning approach," *TURKISH J. Electr. Eng. Comput. Sci.*, vol. 29, nos. 1, pp. 2742–2757, Oct. 2021.
[17] X. Zheng, P. Tang, L. Ai, D. Liu, Y. Zhang, and B. Wang, "White blood cell detection using saliency detection and CenterNet: A two-stage approach," *J. Biophotonics*, vol. 16, no. 3, Mar. 2023, Art. no. e202200174.
[18] D. Yang, H. Zhao, T. Han, Q. Kang, J. Ma, and H. Lu, "Leukocyte subtypes identification using bilinear self-attention convolutional neural network," *Measurement*, vol. 173, Mar. 2021, Art. no. 108643.
[19] M. Hosseini, D. Bani-Hani, and S. S. Lam, "Leukocytes image classification using optimized convolutional neural networks," *Exp. Syst. Appl.*, vol. 205, Nov. 2022, Art. no. 117672.
[20] N. Dong, M.-D. Zhai, J.-F. Chang, and C.-H. Wu, "A self-adaptive approach for white blood cell classification towards point-of-care testing," *Appl. Soft Comput.*, vol. 111, Nov. 2021, Art. no. 107709.
[21] M. Manthouri, Z. Aghajari, and S. Safary, "Computational intelligence method for detection of white blood cells using hybrid of convolutional deep learning and SIFT," *Comput. Math. Methods Med.*, vol. 2022, pp. 1–8, Jan. 2022.
[22] C. Cheuque, M. Querales, R. León, R. Salas, and R. Torres, "An efficient multi-level convolutional neural network approach for white blood cells classification," *Diagnostics*, vol. 12, no. 2, p. 248, Jan. 2022.
[23] Z. Wang, J. Xiao, J. Li, H. Li, and L. Wang, "WBC-AMNet: Automatic classification of WBC images using deep feature fusion network based on focalized attention mechanism," *PLoS ONE*, vol. 17, no. 1, Jan. 2022, Art. no. e0261848.
[24] A. H. Alharbi, C. V. Aravinda, M. Lin, P. S. Venugopala, P. Reddicherla, and M. A. Shah, "Segmentation and classification of white blood cells using the UNet," *Contrast Media Mol. Imag.*, vol. 2022, pp. 1–8, Jul. 2022.
[25] A. Shahzad, M. Raza, J. H. Shah, M. Sharif, and R. S. Nayak, "Categorizing white blood cells by utilizing deep features of proposed 4B-AdditionNet-based CNN network with ant colony optimization," *Complex Intell. Syst.*, vol. 8, no. 4, pp. 3143–3159, Aug. 2022.
[26] A. Çinar and S. A. Tuncer, "Classification of lymphocytes, monocytes, eosinophils, and neutrophils on white blood cells using hybrid AlexNet-GoogleNet-SVM," *Social Netw. Appl. Sci.*, vol. 3, no. 4, pp. 1–11, Apr. 2021.
[27] F. Bozkurt, "Classification of blood cells from blood cell images using dense convolutional network," *J. Sci. Technol. Eng. Res.*, vol. 2, pp. 81–88, Nov. 2021.
[28] L. Jiang, C. Tang, and H. Zhou, "White blood cell classification via a discriminative region detection assisted feature aggregation network," *Biomed. Opt. Exp.*, vol. 13, no. 10, pp. 5246–5260, 2022.
[29] H. Chen, J. Liu, C. Hua, J. Feng, B. Pang, D. Cao, and C. Li, "Accurate classification of white blood cells by coupling pre-trained ResNet and DenseNet with SCAM mechanism," *BMC Bioinf.*, vol. 23, no. 1, pp. 1–20, Dec. 2022.
[30] S. Tavakoli, A. Ghaffari, Z. M. Kouzehkanan, and R. Hosseini, "New segmentation and feature extraction algorithm for classification of white blood cells in peripheral smear images," *Sci. Rep.*, vol. 11, no. 1, pp. 1–13, Sep. 2021.
[31] Z. Han, H. Huang, D. Lu, Q. Fan, C. Ma, X. Chen, Q. Gu, and Q. Chen, "One-stage and lightweight CNN detection approach with attention: Application to WBC detection of microscopic images," *Comput. Biol. Med.*, vol. 154, Mar. 2023, Art. no. 106606, doi: 10.1016/j.compbiomed.2023.106606.

BAIRABOINA SAI SAMBASIVA RAO received the Bachelor of Technology degree in computer science and engineering from K L University, India, in 2017, and the Master of Technology degree in big data analytics from SRM IST, India, in 2019. He is currently pursuing the Ph.D. degree with the School of Computer Science and Engineering, VIT-AP University, India. His research interests include digital image processing, pattern recognition, and deep learning.

BATTULA SRINIVASA RAO is currently an Associate Professor with the School of Computer Science and Engineering, VIT-AP University. His research interests include soft computing, image processing, machine learning, and deep learning.